Gelsolin dysfunction causes photoreceptor loss in induced pluripotent cell- and animal retinitis pigmentosa models

Gelsolin dysfunction causes photoreceptor loss in induced pluripotent cell- and animal retinitis pigmentosa models

Roly Megaw[1], Hashem Abu-Arafeh[1], Melissa Jungnickel[2], Carla Mellough[3], Christine Gurniak-Witke[4], Walter Witke[4], Wei Zhang[5], Hemant Khanna[5], Pleasantine Mill[2], Baljean Dhillon[6], Alan F. Wright[2], Majlinda Lako[3], and Charles ffrench-Constant[1]

[1] MRC Centre for Regenerative Medicine, University of Edinburgh, 5 Little France Drive, Edinburgh EH16 4UU, United Kingdom
[2] MRC Human Genetics Unit, Institute for Genetics and Molecular Medicine, University of Edinburgh, Crewe Road, Edinburgh, EH4 2XU United Kingdom
[3] Institute of Genetic Medicine, Newcastle University, Newcastle, NE1 3BZ, United Kingdom
[4] Institute fur Genetik, Universitat Bonn, Karlrobert-Kreiten-Strasse. 13, 53115, Bonn, Germany
[5] Department of Ophthalmology, UMASS Medical School, 368 Plantation St, Albert Sherman Center, AS6-2043 Worcester, MA 01605
[6] Centre for Clinical Brain Sciences, University of Edinburgh, Chancellors Building, Little France, Edinburgh, EH16 4SB, United Kingdom

Corresponding Author: Roly Megaw roly.megaw@ed.ac.uk

Mutations in the Retinitis Pigmentosa GTPase Regulator (*RPGR*) cause X-linked RP (XLRP), an untreatable, inherited retinal dystrophy that leads to premature blindness. RPGR localises to the photoreceptor connecting cilium where its function remains unknown. Here we show, using murine and human induced pluripotent stem cell models, that RPGR interacts with and activates the actin-severing protein gelsolin, and that gelsolin regulates actin disassembly in the connecting cilium, thus facilitating rhodopsin transport to photoreceptor outer segments. Disease-causing *RPGR* mutations perturb this RPGR-gelsolin interaction, compromising gelsolin activation. Both RPGR and Gelsolin knock out mice show abnormalities of actin polymerization and mislocalization of rhodopsin in photoreceptors. These findings reveal a clinically-significant role for RPGR in the activation of gelsolin, without which abnormalities in actin polymerisation in the photoreceptor connecting cilia cause rhodopsin mislocalisation and eventual retinal degeneration in XLRP. *[135 words]*

The rod photoreceptor enhances processing of visual stimuli by compartmentalising proteins critical for phototransduction within its outer segment (OS). The OS emerges from the distal end of the connecting cilium (CC), with membrane extensions folding to form thousands of disc-like processes that stack to form the body of the OS. The CC is therefore a highly specialised primary cilium whose protein composition is unique to the retina. Up to 10% of OS discs are renewed every day[1] and, with all photoreceptor proteins being synthesised in the cell's inner segment (IS), this high rate of OS turnover requires high levels of protein trafficking from the IS to (and across) the connecting cilium to maintain homeostasis. Indeed, up to 1000 molecules of rhodopsin are trafficked through the 0.3μm-wide connecting cilium in human photoreceptors per second[2]. Breakdown of this cilia trafficking results in protein mislocalisation and, eventually, photoreceptor death. Such photoreceptor degeneration is the hallmark of retinitis pigmentosa (RP)[3], a heterogenous group of inherited retinal dystrophies affecting 1 in 3000 people[4]. RP causes severe visual loss and blindness in middle age. *RPGR* mutations account for 70-90% of XLRP and 10-15% of all RP.[4] Whilst its exact function remains unknown, RPGR localises to the base of the CC where it was proposed to play a role in trafficking of rhodopsin to the OS based on knockout mouse models.[5] Additionally, depletion of *RPGR* in cell lines and mice increases actin polymerization.[6,7] To define RPGR's role in photoreceptor maintenance and to investigate the molecular pathogenesis of XLRP, we generated induced pluripotent stem cells (iPSCs) from patients with *RPGR* type XLRP (*RPGR*/XLRP).

Here, we show *RPGR*-mutant, iPSC-derived photoreceptor cultures display increased actin polymerization, a phenotype also observed in the RPGR knockout mice that show rhodopsin mislocalization and photoreceptor degeneration. RPGR binds to and activates the actin-severing protein gelsolin, an interaction that is lost in RPGR-mutant (XLRP) cells, and Gelsolin knockout mice also show abnormalities of actin polymerization and rhodopsin localization. Activated Gelsolin rescues the ciliogenic defect observed in RPGR-depleted cells. We conclude, therefore, that RPGR mutations in XLRP lead to defective gelsolin activation and defects in actin regulation and rhodopsin trafficking within the photoreceptor connecting cilium.

Results

iPSCs as a novel model for RPGR/XLRP

Induced pluripotent stem cells (iPSCs) were generated from fibroblasts of 2 brothers carrying an *RPGR* mutation (g.ORF15+689_692del4) as previously described[8,9] (Supplementary Fig. 1a and b). Control iPSCs were generated from an unaffected son/nephew. All iPSC clones expressed markers of pluripotency, as demonstrated with qPCR (Supplementary Fig. 1c) and immunostaining (Supplementary Fig. 1d). iPSC lines could differentiate down all three major cell lineages; ectoderm, mesoderm and endoderm (Supplementary Fig. 1e). To generate photoreceptors from these iPSC clones, a 3-dimensional retinal differentiation protocol was optimised.[10,11] (Fig. 1 and Supplementary Fig. 2). Successful patterning of free floating embryoid bodies resulted in spontaneous outpouching of optic vesicles (Fig. 1a-b), which invaginated into optic cup-like structures (Fig. 1c), as previously described.[10] After 100 days, retinal pigment epithelium (RPE) emerged on the outer surface of the cups (Fig. 1d) whilst inside an organised layer of photoreceptors emerged, expressing several maturity-associated markers (Fig. 1e-f). Moreover, while these cells displayed cilia with the classic "9+0" microtubule doublet organization characteristic of primary cilia (Fig. 1g-h) they also were associated with additional membranous, disc-like material produced and deposited between the melanosome-containing RPE cells (Fig. 1j). RPGR, as previously reported[5], localised to this emerging 'connecting cilium' that joins the cell body to the rod outer segment (Fig. 1i). We concluded that human photoreceptors, derived from iPSCs, could therefore be used to study the molecular pathogenesis of *RPGR/*XLRP.

RPGR regulates actin polymerization in hiPS derived and rodent photoreceptors

We first asked whether the abnormalities in the actin cytoskeleton reported in *RPGR*-depleted cell lines[6] are present in iPSC-derived photoreceptors from *RPGR/*XLRP subjects. Increased actin polymerisation was observed in cultured iPSC-derived photoreceptors of both patients compared to the control (Fig. 2a-d, Supplementary Fig 3a). The iPSC-derived *RPGR*/XLRP photoreceptor cultures (CB10 and HB02) showed a 2.7-fold (SEM 0.127; $p<0.0001$, n=3) and 2.49-fold (SEM 0.34; $p=0.0081$, n=3) increase in actin polymerisation respectively, compared with the control line (MB02), as determined by quantitative imaging of phalloidin staining (unpaired, two-tailed t-test). As an alternative method of confirming a cytoskeletal abnormality, iPSC-derived photoreceptor cultures were screened for phosphorylation levels of 639 phosphoproteins (Fig. 2e). Unbiased proteomic analysis of *RPGR*/XLRP and control lines revealed a significant increase in phosphorylation of cytoskeletal regulatory proteins in the diseased photoreceptor cultures as compared to control. The mean ratio of phosphorylation level in diseased versus control cells was 0.092 +/- 0.0033 (n=56 proteins) compared with non-cytoskeletal proteins (-0.008 +/- 0.01, n=583 proteins, $p=0.004$) (Fig. 2e, Supplementary Data 1). These results further support a disruption of cell signaling pathways regulating actin turnover in *RPGR*/XLRP mutant photoreceptors.

In parallel experiments to confirm a role for RPGR in actin turnover in the photoreceptor connecting cilium *in vivo*, we examined a recently reported *Rpgr* knockout (KO) mouse.[12] Significant photoreceptor degeneration was observed by 4 months of age (Fig. 3a-c). Prior to this, at 3 weeks of age, signs of photoreceptor stress were apparent as evidenced by increased GFAP immunolabeling throughout the radial length of Müller cells in the outer nuclear layer (ONL: Fig. 3d). Additionally, the photoreceptors failed to correctly localise rhodopsin to the outer segment at this stage: instead it was trafficked to the outer plexiform layer and eventually remained in the peri-nuclear space (Fig. 3e-f). Cytoskeletal examination in murine retina during development (at postnatal day 2 and 10) revealed no difference between wild type and *Rpgr* KO photoreceptors (Supplementary Fig. 4), suggesting the initial photoreceptor development was RPGR-independent at stages where neonatal eyes are still closed and phototoxicity minimal. The degeneration in *Rpgr*-mutant photoreceptor seems to be linked to when eyes open at P14, as reactive gliosis is detected by P21 and by 2 months of age, increased actin polymerisation was seen in the connecting cilia (Fig. 3g), all prior to photoreceptor loss. These results demonstrate that RPGR is required for actin regulation in the mature photoreceptor connecting cilium and for correct localisation of rhodopsin to its outer segment *in vivo*.

RPGR mutations ameliorate the activation of the actin severing protein Gelsolin

Next, we performed a cytoskeletal-focused phosphoarray in an attempt to determine the mechanism by which RPGR regulates actin turnover. We observed in *RPGR*/XLRP photoreceptor cultures that cofilin, a protein whose role in regulating actin polymerization appears important for ciliogenesis[13] and which localizes to the photoreceptors in mature wild type retina (Supplementary Fig 5), showed 3.16-fold higher levels of phosphorylation of Serine 3, a post-translational modification that inhibits binding to and treadmilling/depolymerisation of F-actin[14] (Fig. 4a). This result was confirmed by western blot analysis of repeat cultures of both *RPGR*/XLRP lines compared to control (Fig. 4b; Blot Density Measurement Control MB02 22.544% v Patient CB10 40.364% v Patient HB02 37.092%). This post-translational modification of cofilin is normally inhibited by the actin-severing protein gelsolin[15], suggesting that loss of gelsolin activity might be responsible for the increased actin polymerization and photoreceptor abnormalities seen in the *RPGR*-mutant photoreceptors. In support of this, it has been shown that fibroblasts from *gelsolin* knockout mice show similar increased actin fibre formation[16] as seen in our cultured iPSC-derived *RPGR*/XLRP photoreceptors and *RPGR*-knockdown lines.[6] Moreover, gelsolin has been shown to regulate cilia formation, as evidenced by degeneration of outer ear stereocilia in *gelsolin* KO mice[17] and the identification of gelsolin in an siRNA screen for genes required in ciliogenesis.[18] We therefore examined gelsolin activation in human *RPGR*/XLRP photoreceptors. Gelsolin occurs in two forms; a closed, inactive conformation in which the N- and C-terminal halves bind to each other, and an open, active conformation in which the N-terminal half binds to and cleaves actin filaments.[19,20] The two forms can be separated by biochemical isolation of F-actin, to which only the activated form will bind.[21,22] When F-actin was isolated from our cultures, it revealed decreased levels of bound (active) gelsolin in *RPGR*/XLRP iPSC-derived photoreceptors from both XLRP subjects compared to control photoreceptors, despite increased levels of the polymerized F-actin substrate (Fig. 4c; Blot Density Measurement Control MB02 15.507% v Patient CB10 7.316% v Patient HB02 8.012%, Supplementary Fig 3b). These observations show that *RPGR*/XLRP mutations attenuate gelsolin activation with subsequent disruption of its downstream pathways.

Gelsolin KO mice phenocopy the retinal abnormalities seen in _Rpgr_ KO mice

To confirm that the increased actin polymerization and rhodopsin mislocalization observed in *Rpgr* KO photoreceptors could be the consequence of loss of gelsolin activity, we examined the retina of the *gelsolin* KO mouse.[16] At 5 months of age, a similar phenotype was seen, with rhodopsin mislocalisation to the outer plexiform layer and peri-nuclear space (Fig. 5a). Increased GFAP immunolabeling throughout the radial length of Müller cells in the ONL was observed (Fig. 5d). Further, degeneration of the photoreceptor-containing ONL was significant by 5 months of age (Fig. 5b-c). At earlier time points (2 months old), increased actin polymerisation was seen in the connecting cilia (Fig. 5e), akin to the *Rpgr* KO mouse. Together, these observations show that gelsolin regulates actin polymerization in the photoreceptors and is required for both rhodopsin transport to the photoreceptor outer segment and photoreceptor maintenance.

RPGR binds gelsolin and activated gelsolin can rescue _RPGR_-deficient cells

Having established that loss of gelsolin phenocopies key abnormalities of the *Rpgr* KO mouse, we next sought to determine whether there is a direct biochemical interaction between RPGR and gelsolin. Co-immunoprecipitation (Co-IP) of recombinant proteins revealed that gelsolin binds directly to the ubiquitous splice variant ($RPGR^{Ex1-19}$) but not the retina-enriched $RPGR^{ORF15}$ form of the protein (Supplementary Fig. 6). To confirm the RPGR-gelsolin interaction *in vivo*, co-IP and reverse co-IP using bovine retinal extract were performed. These experiments revealed such an interaction between the two proteins *in vivo* (Fig. 6a), as did endogenous co-IP of protein product from photoreceptor cultures derived from our control iPSC lines (Fig. 6b). In these endogenous retinal extracts, however, both the ubiquitous splice variant ($RPGR^{Ex1-19}$) and the retina-enriched $RPGR^{ORF15}$ isoforms were pulled down with gelsolin. Importantly, this interaction was disrupted in photoreceptor cultures derived from both our *RPGR*/XLRP iPSC lines (Fig. 6b), with both the ubiquitous splice variant ($RPGR^{Ex1-19}$) and the retina-specific $RPGR^{ORF15}$ forms of the protein no longer binding to gelsolin in the presence of the mutation in the latter. Thus RP-causing mutations in the retinal-specific $RPGR^{ORF15}$ block the interaction of the ubiquitous $RPGR^{Ex1-19}$ isoform with gelsolin, resulting in reduced gelsolin activation and impaired F-actin turnover.

If the RPGR-gelsolin interaction were responsible for regulating gelsolin activity, and thus actin polymerization in the photoreceptor, we would predict that the consequences of *Rpgr* loss could be rescued by expression of activated gelsolin. To test this, we examined an easily-quantifiable reporter of

RPGR function; the inhibition of ciliogenesis induced by serum starvation in *RPGR*-depleted hTERT-RPE cells (Fig. 6c-e) as previously described.[6] Concurrent expression of the active, N-terminal half of gelsolin[23] in this cell line restored cilia formation to wild type levels (Fig. 6d-e), confirming that gelsolin activation can rescue *RPGR* loss.

Discussion

This report shows that RPGR functions in photoreceptors to activate the actin-cleaving protein gelsolin, since KO mice lacking gelsolin showed the same retinal phenotype as *RPGR* KO mice and human XLRP mutations in *RPGR* prevented the normal interaction between RPGR and gelsolin, reducing its activation and increasing actin polymerization. Further support for the significance of this interaction comes from a report that families with a homozygous D187N (G654A) mutation in the human gelsolin (*GSN*) gene have RP, as well as manifestations of systemic amyloidosis[24] resulting from either loss-of-function (e.g. RP) or deposition of amyloidogenic gelsolin fragments.

This activation of gelsolin is achieved by direct binding to RPGR, as evidenced by Co-IP studies showing the interaction of gelsolin with RPGR and by disruption of both this binding and subsequent activation of gelsolin in the presence of an XLRP mutation. Our results suggest the primary binding site appears to be in the ubiquitous splice variant ($RPGR^{Ex1-19}$) rather than the retina-specific $RPGR^{ORF15}$ isoform. The finding that the pathogenic mutation that prevents this binding is in the $RPGR^{ORF15}$ isoform could be explained by the finding that the two RPGR isoforms form a complex *in vivo* (WZ and HK, unpublished observations), whereupon the mutant $RPGR^{ORF15}$ prevents gelsolin binding to the $RPGR^{Ex1-19}$ isoform.

There are two potential mechanisms by which the dysregulation of actin caused by abnormalities of gelsolin activation could lead to the mislocalisation of rhodopsin, photoreceptor stress and eventual degeneration characteristic of XLRP (Fig. 7). Firstly, by disturbing cilia formation, which impacts on the genesis and maintenance of the modified cilium that comprises the photoreceptor. It is well recognised that actin exerts an influence on ciliogenesis and cilia maintenance.[18,25,26,27] Indeed, actin depolymerisation leads to lengthened, nascent, outer segment discs in photoreceptors.[28,29] Actin is localized to the distal portion of the connecting cilium in human photoreceptors where the ciliary membrane evaginates to form outer segment discs.[30,31] These results suggest that RPGR facilitates outer segment disc budding or the completion of disc formation by locally regulating actin dynamics in a gelsolin-dependent manner. In keeping with this, the disorganised nature of discs reported in an *Rpgr* KO mouse[5] occurs with a hyperstabilized actin cytoskeleton in both mutant postnatal mouse eyes and *RPGR* mutant photoreceptor organoids charaterized here. Additional support comes from a role of RPGR in facilitating the outer segment content of inositol polyphosphatase INPP5E.[32] INPP5E regulates the phosphoinositide content of the membrane, which in turn regulates the local lipid-actin cytoskeleton interface.[33] Excitingly, recent work has demonstrated the highly-localized role actin plays in excision of a membranous bud (ectosome) at the cilia tip.[34,35] The process, known as ectocytosis (or decapitation), serves as an alternative ciliary exit route for G-protein coupled receptors. We speculate that photoreceptor disc formation may share a common ancestral mechanism with ectocytosis and that RPGR's alternatively spliced ORF15 variant may have evolved to facilitate this.

Secondly, photoreceptor degeneration could occur if actin dysregulation functionally abrogates rhodopsin trafficking. In the photoreceptor, an actin bundle connects the periciliary membrane complex with the basal body at the base of the connecting cilium, along which the actin-based motor protein myosin VIIA appears to travel.[29,36] Myosin VIIa contributes to the active transport of visual pigments, including rhodopsin, into the connecting cilium.[36] Support for a role of RPGR and gelsolin in ciliary function and rhodopsin trafficking comes from work examining Usher Syndrome, a syndromic form of RP and deafness. This syndrome can be caused by *whirlin* (*WHRN*) mutations[37], coding for a protein that forms part of the usherin complex that regulates the actin filament network in the periciliary membrane complex.[38,39] Gelsolin is part of this WHRN complex in inner ear stereocilia[17] where it is mislocalised away from stereocilia in the *whirlin* mutant mouse.[17] WHRN has also been shown to interact with the RPGR ORF15 basic domain in photoreceptors[40], in keeping with a model whereby loss of WHRN perturbs the regulation of gelsolin-mediated actin turnover by RPGR, disrupting myosin VIIa-mediated rhodopsin transport at the periciliary membrane complex. RPGR also facilitates the ciliary targeting of the small G protein, RAB8,[41] which regulates vesicular trafficking during primary ciliogenesis and rhodopsin transport in the photoreceptor,[42] supporting this model.

These models are not mutually exclusive, and further work will define their relative contributions to the pathology of XLRP as well as addressing the important translational implication of our study that pharmacomodulation or ectopic expression of activated gelsolin in the retina could slow or reverse the retinal degeneration observed in *RPGR*/XLRP disease.

Methods

Antibodies and reagents

Primary antibodies: mouse anti-OCT3/4 (R&D AF1759 10ug/ml IF), goat anti-Nanog NL493-conjugated (R&D 967151; 1 in 10 IF), SOX2 (eBioscience 14-9811-82; 1 in 100 IF), rabbit anti-SMA (Abcam AB5694; 1 in 100 IF), β-Tub (Abcam ab7751; 1 in 1000 IF), mouse anti-αFP (Sigma A8452; 1 in 500 IF), rabbit anti-PAX6 (Covance PRB-278P; 1 in 200 IF), goat anti-CHX10 (Santa Cruz SC-21692; 1 in 500 IF), rabbit anti-RPGR (Atlas Antibodies HPA001593; 1 in 200 IF), rabbit anti-Recoverin (Chemicon AB5585; 1 in 100 IF), mouse anti-RETP1 (Chemicon MAB5326; 1 in 1000 IF), phalloidin-Alexa647 (Life Technologies a2287; 1 in 200 IF), Hoechst, rabbit anti-GFAP (DAKO ZO334; 1 in 100 IF), mouse anti-acetylated α-tubulin (Sigma, T6793; 1 in 200 IF), rabbit anti-Gelsolin (Abcam 74420; 1 in 900 WB), rabbit anti-Cofilin/pCofilin (Cell Signalling 3313 & 5175; 1 in 1000 WB), mouse anti-GAPDH (Chemicon MAB374; 1 in 1000 WB)

Secondary antibodies (all Life Technologies; all 1 in 1000 dilution unless otherwise stated): donkey anti-mouse-Alexa488 (A21202), donkey anti-mouse-Alexa568 (A10037), donkey anti-goat-Alexa488 (A21432), donkey anti-goat-Alexa555 (A11055), donkey anti-sheep-Alexa488 (A11015), donkey anti-sheep-Alexa568 (A21099), donkey anti-rabbit-Alexa488 (A10042), donkey anti-rabbit-Alexa568 (A21206), Horseradish peroxidase rabbit (NA934V, GE Healthcare; 1 in 10000 WB) or Mouse (NA931V, GE Healthcare; 1 in 10000 WB).

siRNA duplexes (all with dT overhangs) were purchased from Sigma-Aldrich: control siRNA: 5'-UUCUCCGAACGUGUCACGU-3'; *RPGR* siRNA: 5'-GAGAUAGAUAAUUCUUCAA-3'.[6] Constitutively active gelsolin (Ch-*gelsolN*) was a gift from Ikuo Wada (Addgene plasmid # 37262)[23].

iPSC Generation

Skin biopsies were performed under local anaesthetic (Xylocaine 2% with Adrenaline 100 micrograms/20 ml (1:200,000), AstraZeneca) using a sterile technique following ethical approval (REC Ref No 10/S1103/10, Lothian R&D Project No 2012/R/DER/01) and informed consent. Both patients and controls were aware of their use of their samples in research. Fibroblast cell lines developed in Dubecco's Modified Eagle Medium (Gibco) with 10% fetal calf serum (Gibco) and 1:500 Penicillin/Streptomycin (Gibco).

Three micrograms of expression plasmid mixtures (generous donation from Yamanaka lab)[8] were electroporated into 500,000 fibroblasts in Amaxa Nucleofector 2b (Lonza AAB1001) according to the manufacturer's instructions and transferred to a 6-well Gelatin-coated plate (1% Sigma) in DMEM/10% FCS. The cells were trypsinized upon reaching confluence and replated on Geltrek in Essential8 media[43] (E8; Gibco) in a 100ml dish. Colonies were counted after 25 days and hESC-looking colonies picked and expanded. Cells were maintained on Geltrek in E8 and passaged with EDTA (0.5M, Invitrogen).

Photoreceptor differentiation

3 dimensional optic cup structures protocols were adapted from previous protocols.[10,11] Confluent iPSC colonies were dissociated using EDTA (0.5M, Invitrogen), resuspended in Essential6 media (Gibco) and allowed to form embryoid bodies in non-adherent 10cm petri dishes (Sterilin) at 37^{o}C on an orbital shaker (Stuart). 24 hours later they began patterning for 12 days with reducing knockout serum replacement (KOSR; 20% for 5 days, 15% until day 9, 10% until day 37), 1:50 B27 (PAA), 5ng/ml rhIGF-1 (Sigma), 3um IWR1e and 1% Geltrek in DMEM/Ham's F-12 (Gibco). From day 12 to 18, cultures were incubated with reducing KOSR, 1:50 B27 (PAA), 5ng/ml rhIGF-1 (Sigma), 10% FCS, 100nm SAg and 1% Geltrek in DMEM/Ham's F-12 (Gibco). From day 18 to 37, DMEM: F-12 was supplemented with 10% KOSR, 1:50 B27 (PAA), 5ng/ml rhIGF-1 (Sigma) and 1% Geltrek. From Day

37 onwards, DMEM: F-12 was supplemented with 1:50 B27 (PAA), 1:100 N2 (Gibco), 10ng/ml rhIGF-1 (Sigma) and 1% Geltrek.

Animals

All experiments were performed in compliance with the ARVO Statement for the Use of Animals in Ophthalmic and Vision Research, and the United Kingdom Animals (Scientific Procedures) Act 1986 under project licence number P8C815DC9 (Dr X Shu).

Histology and Immunostaining

Mouse eyes[12,16] were fixed immediately after enucleation and corneal excision in 4% paraformaldehyde (Sigma-Aldrich) in PBS at room temperature (RT) for 1 hour, infiltrated with sucrose for cryoprotection (15%, 30%) and embedded in OCT (CellPath). Complete sectioning of whole eyes was performed through the horizontal meridian. Sections (8-50μm thickness) were collected. 3-dimensional iPSC-derived optic cup structures were fixed, cryoprotected, embedded and sectioned in a similar fashion. hTERT-RPE cells grown on slides were fixed in 4% paraformaldehyde for 30 min at RT.

Sections/cells were blocked/permeabilized with 2% NDS (Sigma), 2% BSA (Sigma) and 0.5% Triton X-100 (Fisher) for 1 hour at RT, washed with PBS, incubated with primary antibodies overnight at 4^{o}C, washed in PBS, incubated with secondary antibodies for 60min at RT, washed in PBS, incubated in Phalloidin for 30mins at RT, washed in PBS, incubated in Hoechst for 5mins at RT and mounted with coverslips using Fluoromount-G (Southern Biotech). Images were taken on Leica SPE confocal microscope and analysed using the ImageJ and ImagePro software. Images represent confocal projections, unless stated otherwise.

For actin levels, pixel intensity of phalloidin staining of standardised regions of interest (ROI) of confocal Z-stacks were measured by blinded assessors using ImageJ.

Assessors were blinded for all mouse retina measurements.

Electron Microscopy

3-dimensional optic cup-structures were fixed in 2.5% Glutaraldehyde (TAAB) in 0.1M Phosphate (PO) buffer at RT (2 hours), washed (0.1M PO buffer) and lipids stained with 1% Osmium Tetroxide (Electron Microscopy Science) (1 hour). Samples were washed (PO buffer) prior to ethanol dehydration. Residual ethanol was removed with propylene oxide (TAAB) prior to overnight incubation in 5g Araldite CY212 (Agar Scientific) and 5g Dodecenyl Succinic Anhydride (DDSA, Agar Scientific). Sequential incubations in the above mix preceded transfer to final embedding resin (11.5g Araldite CY212, 11g DDSA, 0.55mls Benzyldimethylamine (Agar Scientific), 0.5mls Dibutylphthalate (Agar Scientific). Repeated exchange of embedding resin preceded 48 hours in an oven (60^{o}C).

RNA extraction and RT–PCR

mRNA was extracted from transfected cells using the RNeasy Minikit (Qiagen, Crawley, UK) before being reverse transcribed with the Superscript First Strand Synthesis System for RT-PCR (Invitrogen) as per manufacturer's instructions. The resulting cDNA was used to perform RT-PCR with the Roche Light Cycler 480 II using the QuantiFast SYBR Green PCR Kit (Qiagen) and the following primers: *L-MYC* : Fd CAGGGGGTCTGCTCGCACCGTGATG & Rv TCAATTCTGTGCCTCCGGGAGCAGGGTAGG; *OCT3/4* : Fd GTTGGAGAAGGTGGAACCAA & Rv CTCCTTCTGCAGGGCTTTC; SOX2 : Fd GTGTTTGCAAAAAGGGAAAAGT & Rv TCTTTCTCCCAGCCCTAGTCT; *LIN28* : Fd AGCCATATGGTAGCCTCATGTCCGC & Rv TCAATTCTGTGCCTCCGGGAGCAGGGTAGG; *PAX6* : Fd CTCGGTGGTGTCTTTGTCAAC & Rv ACTTTTGCATCTGCATGGGTC; *Rx* : Fd GAATCTCGAAATCTCAGCCC & Rv CTTCACTAATTTGCTCAGGAC; *LHX2* : Fd CAAGATCTCGGACCGCTACT & Rv CCGTGGTCAGCATCTTGTTA; *SIX3* : Fd CCGGAAGAGTTGTCCATGTT & Rv CGACTCGTGTTTGTTGATGG; *SIX6* : Fd ATTTGGGACGGCGAACAGAAGACA & Rv ATCCTGGATGGGCAACTCAGATGT; *CRX* : Fd GTGAGGAGGTGGCTCTGAAG & Rv

CTGCTGTTTCTGCTGCTGTC; *NESTIN* : Fd CAGGAGAAACAGGGCCTACA & Rv TGGGAGCAAAGATCCAAGAC; *ARRESTIN* : Fd CTACCTGGGGAAACGGGACT & Rv GGCCATAGCGAAAGGCACA; *RECOVERIN* : Fd TTCAAGGAGTACGTCATCGCC & Rv GATGGTCCCGTTACCGTCC

Western blots

Cells were lysed on ice in Pierce RIPA Buffer (ThermoScientific) containing Protease (Millipore) and Phosphatase (Calbiochem) inhibitors. Lysates were centrifuged (16000g) for 10 min and the post-nuclear supernatants were incubated for 5 min at 95^{o}C with Laemmli sample buffer. Proteins were separated on a 4-20% Precise Tris-HEPES Protein Gel (ThermoScientific) and transferred to an Immobilon P Membrane (Merck Millipore). Blots were blocked in milk for 1hr before incubation with primary antibodies overnight in 4% BSA . A secondary antibody coupled with horseradish peroxidase was used for detection by a Licor C-Digit digital reader or a Konika Minolta SRX-101A developer with Super RX-N film (FujiFilm). All uncropped western blots can be found in supplementary figure 7.

Coimmunoprecipitation of Bovine retina and iPSC cultures

Bovine retina and photoreceptor cultures were lysed on ice with buffer (1% Triton-X100, 50mMol Tris and 150mMol NaCl in PBS (pH7.4)) containing Protease (Millipore) and Phosphatase (Calbiochem) inhibitors. Lysates were centrifuged (16000g) for 10 min. Antibody was attached to Dynabeads Protein A (Life Technologies) and immunoprecipitation performed as per manufacturer's instructions. Supernatants were incubated for 10 min (70^{o}C) with Laemmli sample buffer. Proteins were separated on 4-20% Precise Tris-HEPES Protein Gel (ThermoScientific) and transferred to an Immobilon P Membrane (Merck Millipore). Blots were blocked in milk and incubated with primary antibodies overnight in 4% BSA . Secondary antibody coupled with horseradish peroxidase was used for detection by a Licor C-Digit digital reader or a Konika Minolta SRX-101A developer with Super RX-N film (FujiFilm).

Coimmunoprecipitation of Recombinant Proteins

Cell Culture, Transient transfection and co-IP: hTERT-RPE1 cells were maintained in DMEM/F12 (Invitrogen) plus 10% FBS and penicillin/streptomycin. For testing Gelsolin-RPGR interaction, we transiently transfected the cells with plasmids encoding FLAG-tagged Gelsolin and GFP-tagged full length $RPGR^{Ex1\text{-}19}$ (const), $RPGR^{ORF15}$ and different RPGR domains ($RPGR^{1\text{-}11}$, $RPGR^{1\text{-}15}$, $RPGR^{12\text{-}15}$, or $RPGR^{16\text{-}19}$). Details of these constructs have been described previously.[41] At the end of 48h, cells were lysed in IP lysis buffer [25mM Tris PH 7.4, 150 mM NaCl, I mM EDTA, 1% NP-40, 5% Glycerol and Complete Protease Inhibitor (Roche)]. The lysates were centrifuged to remove the debris and subjected to pulldown using GFP antibody crosslinked to AminoLink Plus Coupling Resin. The details of crosslinking have been described.[32] The immunoprecipitate was washed three times with the IP lysis buffer and the samples were eluted in glycine lysis buffer (pH 2.8), neutralized using 1M Tris pH 9.5 and analysed by SDS-PAGE and immunoblotting.

Gelsolin Assay for determination of triton-insoluble F-actin

Cell cultures were lysed with buffer containing 120mM PIPES, 50mM HEPES, 4mM MgCl2, 10mM Glucose, 20mM EDTA, 0.1mM Dithiothreitol, 1mM Phenylmethylsulfonylfluoride and Protease (Millipore) and Phosphatase (Calbiochem) inhibitors. Initial lysate also contained 1.5% Triton-X100 to isolate Triton-soluble G Actin (inactive/unbound Gelsolin).[21,22] Lysate was vortexed (10 mins) and spun (12000g) for 10mins, all at 4^{o}C. Triton-soluble supernatant (G actin; inactive/unbound Gelsolin) was removed and the pellet resuspended in lysis buffer containing 6% SDS prior to 10 mins vortexing and centrifugation (12000g) for 10 mins, all at RT. Resulting supernatant contained F actin (active/bound gelsolin). Lysates were then processed for western blotting.

Phospho protein arrays

Arrays were carried out as per manufacturer's instructions (Fullmoon Bio). Briefly, 100 day old photoreceptor cultures (RPGR mutant v Control, n=1) were lysed with extraction buffer containing Protease (Millipore) and Phosphatase (Calbiochem) inhibitors, purified and biotinylated. Array chips were blocked and biotinylated proteins allowed to couple to chips. Chips were washed, incubated with

Cy3 streptavidin, washed and measured on Axon 4200A slide scanner.

Transfection and cilia formation

Cells were transfected with Lipofectamine2000 (Invitrogen) using the reverse transfection protocol as per manufacturer's instructions. 0.125ul control/*RPGR* siRNA[1] and 1ul Lipofectamine2000 were diluted in 100ul OptiMEM (Gibco) and incubated for 20mins in a 24-well plate at RT. Cells were plated on the siRNA/Lipofectamine mix at $3x10^4$ cells/well. 24 hours later the siRNA/Lipofectamine mix was removed and replaced by 2ul *Ch-gelsolN*[23], 2ul Lipofectamine and 100 OptMEM (preincubated for 20mins at RT). 4 hours later, the medium was replaced with serum-free medium for 24h, after which cells were fixed, immunostained and assessed for cilia formation.

Data Availability

All data generated or analysed during this study are included in this published article (and its supplementary information) or from the corresponding author upon reasonable request.

Acknowledgements

We would like to acknowledge Dr Xinhua Shu (University of Caledonia) for kindly housing the Rpgr ko mice. We would also like to thank CB, HB, MB and KR for their generous tissue donation to generate the iPSCs.

Author Contributions

R.M., A.W.F., M.L. and C. ff-C. designed research; R.M., H. A-A., M. J., C. G-W. and W. Z. performed research. R.M., H. A-A., M. J., C. M., H. K., P.M., M.L., C. ff-C. analysed data; R.M. and C. ff-C. wrote the manuscript; R.M., C. M., W.W., H. K., P.M., B.D. A.W.F., M.L. and C. ff-C edited the manuscript.

Competing Financial Interests

The authors declare no competing financial interests

References

1. Young R.W. The renewal of photoreceptor cell outer segments. J. Cell Biol. 33, 61-72 (1967).
2. Besharse J.C. Photosensitive membrane turnover: Differentiated membrane domains and cell–cell interaction. In R. Adler & D. Farber (Eds.), The retina: A model for cell biological studies (pp. 297–352). (1986).
3. Megaw R., Soares D. & Wright A.F. RPGR: Its role in photoreceptor physiology, human disease, and future therapies. Exp. Eye Res. 138, 32-41 (2015).
4. Wright A.F., Chakarova C.F., Abd El-Aziz M.M. & Bhattacharya, S.S. Photoreceptor degeneration: genetic and mechanistic dissection of a complex trait. Nat. Rev. Genet. 11, 273-84 (2010).
5. Hong D. et al. A retinitis pigmentosa GTPase regulator (RPGR)-deficient mouse model for X-linked retinitis pigmentosa (RP3). Proc. Natl. Acad. Sci. USA 97, 3649-3654 (2000).
6. Gakovic M. et al. The role of RPGR in cilia formation and actin stability. Hum. Mol. Gen. 20, 4840-50 (2011).
7. Takahashi K. et al. Induction of pluripotent stem cells from adult human fibroblasts by defined factors. Cell 131, 861-72 (2007).
8. Okita K. et al. A more efficient method to generate integration-free human iPS cells. Nat. Methods 8, 409-12 (2011).
9. Nakano T. et al. Self-formation of optic cups and storable stratified neural retina from human ESCs. Cell Stem Cell 10, 771-85 (2012).
10. Mellough C. et al. IGF-1 Signaling Plays an Important Role in the Formation of Three-Dimensional Laminated Neural Retina and Other Ocular Structures From Human Embryonic Stem Cells. Stem Cells 33, 2416-30 (2015).
11. Huang W.C. et al. RPGR-associated retinal degeneration in human X-linked RP and a murine model. Invest. Ophthalmol. Vis. Sci. 53, 5594-5608 (2012).
12. Zhang C. et al. NudC regulates actin dynamics and ciliogenesis by stabilizing cofilin 1. Cell Res. 26, 239-53 (2016).
13. Ressad F. et al. Kinetic Analysis of the Interaction of Actin-depolymerizing Factor (ADF)/Cofilin with G- and F-Actins. J. Biol. Chem. 273, 20894-902 (1998).
14. Takahashi K., Kanno SI. & Mizuno K. Activation of cytosolic Slingshot-1 phosphatase by gelsolin-generated soluble actin filaments. Biochem. Biophys. Res. Commun. 454, 471-477 (2014).
15. Witke W. et al. Hemostatic, inflammatory, and fibroblast responses are blunted in mice lacking gelsolin. Cell 81, 41-51 (1995).
16. Mburu P. et al. Gelsolin plays a role in the actin polymerization complex of hair cell stereocilia. PLoS One. 5, e11627 (2010).
17. Kim J. et al. Functional genomic screen for modulators of ciliogenesis and cilium length. Nature 464, 1048–1051

(2010).
18. Cooper J. et al. Microinjection of gelsolin into living cells. J. Cell Biol. 104, 491-501 (1987).
19. Burtnick L., Urosev D., Irobi E., Narayan K. & Robinson R. Structure of the N-terminal half of gelsolin bound to actin: roles in severing, apoptosis and FAF. The EMBO Journal 23, 2713-2722 (2004).
20. Cunningham C. et al. Cell permeant polyphosphoinositide-binding peptides that block cell motility and actin assembly. J. Biol. Chem. 276, 43390-43399 (2001).
21. Finkelstein M., Etkovitz N. & Breitbart H. Role and Regulation of Sperm Gelsolin Prior to Fertilization. J. Biol. Chem. 285, 39702-39709 (2010).
22. Nagaya H. et al. Regulated motion of glycoproteins revealed by direct visualization of a single cargo in the endoplasmic reticulum. J. Cell Biol. 180, 129-143 (2008).
23. Ardalan MR., Shoja MM. & Kiuru-Enari S. Amyloidosis-related nephrotic syndrome due to a G654A gelsolin mutation: the first report from the Middle East. Nephrol. Dial .Transplant 22, 272-5 (2007).
24. Bershteyn., M Atwood SX., Woo WM., Li M. & Oro AE. MIM and cortactin antagonism regulates ciliogenesis and hedgehog signaling. Dev. Cell 19, 270-83 (2010).
25. Kim J., Jo H., Hong H., Kim MH., Kim JM., Lee JK., Heo WD. & Kim J. Actin remodelling factors control ciliogenesis by regulating YAP/TAZ activity and vesicle trafficking. Nat. Commun. 7, 6781 (2015).
26. Miyatake K., Kusakabe M., Takahashi C. & Nishida E. ERK7 regulates ciliogenesis by phosphorylating the actin regulator CapZIP in cooperation with Dishevelled. Nat. Commun. 6, 6666 (2015).
27. Vaughan DK. & Fisher SK. 1989. Cytochalasin D disrupts outer segment disc morphogenesis in situ in rabbit retina. Invest. Ophthalmol. Vis. Sci. 30, 339-42. (1989).
28. Williams DS., Linberg KA., Vaughan DK., Fariss RN. & Fisher SK. Disruption of microfilament organization and deregulation of disk membrane morphogenesis by Cytochalasin D in rod and cone photoreceptors. J. Comp. Neurol. 272, 161- 176 (1988).
29. Arikawa K & Williams DS. Organization of actin filaments and immunocolocalization of alpha-actinin in the connecting cilium of rat photoreceptors. J. Comp. Neurol. 288, 640-6 (1989).
30. Chaitin M. & Burnside B. Actin filament polarity at the site of rod outer segment disk morphogenesis. Invest. Ophthalmol. Vis. Sci. 30, 2461-9 (1989).
31. Nager AR. et al. An Actin Network Dispatches Ciliary GPCRs into Extracellular Vesicles to Modulate Signaling. Cell 168, 252-263 (2017).
32. Phua SC. et al. Dynamic Remodeling of Membrane Composition Drives Cell Cycle through Primary Cilia Excision. Cell 168, 264-279 (2017).
33. Wolfrum U. & Schmitt A. Rhodopsin transport in the membrane of the connecting cilium of mammalian photoreceptor cells. Cell Motil. Cytoskeleton 46, 95 - 107 (2000).
34. Ebermann I. et al. A novel gene for Usher syndrome type 2: mutations in the long isoform of whirlin are associated with retinitis pigmentosa and sensorineural hearing loss. Hum. Genet. 121, 203-11 (2007).
35. Wang L. et al. Whirlin interacts with espin and modulates its actin-regulatory function: an insight into the mechanism of Usher syndrome type II. Hum. Mol. Genet. 21, 692-710 (2012).
36. Maerker T. et al. A novel Usher protein network at the periciliary reloading point between molecular transport machineries in vertebrate photoreceptor cells. Hum. Mol. Genet. 17, 71-86. (2008).
37. Wright RN., Hong D. & Perkins B. RpgrORF15 connects to the Usher protein network through direct interactions with multiple whirlin isoforms. Invest. Ophthalmol. Vis. Sci. 53, 1519-29 (2012).
38. Murga-Zamalloa C. et al. Interaction of retinitis pigmentosa GTPase regulator (RPGR) with RAB8A GTPase: implications for cilia dysfunction and photoreceptor degeneration. Hum. Mol. Genet. 19, 3591–3598 (2010).
39. Moritz OL. et al. Mutant rab8 Impairs Docking and Fusion of Rhodopsin-bearing Post-Golgi Membranes and Causes Cell Death of Transgenic *Xenopus* Rods. Mol. Biol. Cell 12, 2341–2351 (2001).
40. Chen G. et al. Chemically defined conditions for human iPSC derivation and culture. Nat. Methods 8, 424-9 (2011).
41. Rao KN. et al. Prenylated retinal ciliopathy protein RPGR interacts with PDE6™ and regulates ciliary localization of Joubert Syndrome-associated protein INPP5E. Hum. Mol. Genet. 25, 4533-4545 (2016).

Figures

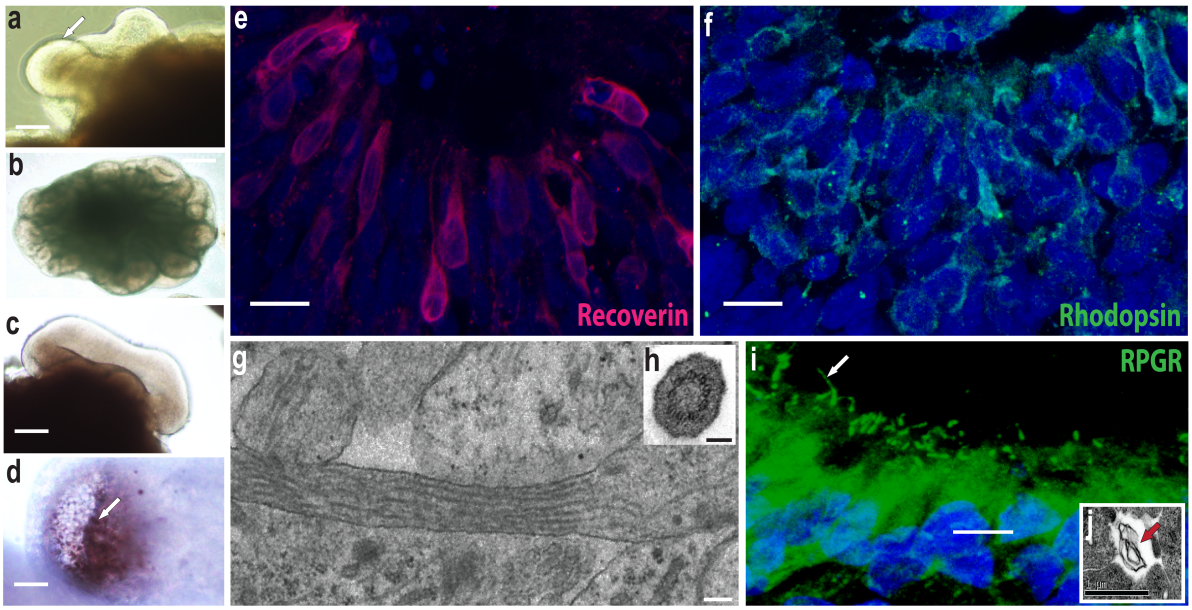

Figure 1. 3-dimensional patterning of induced pluripotent stem cells produces mature photoreceptors Free floating aggregates grown using a retinal differentiation protocol[9,10] self-organise into budding spheroids with a single bud shown in **a** (arrow) and multiple buds from one spheroid in **b**. Buds invaginate (**c**) to form optic cups which mature over 100 days (**d**). Pigmented retinal pigment epithelium (RPE) emerges externally (arrow; **d**) whilst a radial arrangement of Recoverin (**e**) and Rhodopsin (**f**) expressing photoreceptors organise internally, forming an outer nuclear-like layer. Electron microscopy studies reveal a classic "9+0" microtubule doublet formation in these cilia (**g,** inset **h** shows cross-section). RPGR is present in photoreceptor cilia (arrow; **i**) whilst electron microcopy shows the production of membranous material, as required for outer segment formation (arrow, **j**). Scale bars: 400µm (b); 200µm (a); 50µm (c,d); 10µm (e,f); 100nm (g); 200nm (h); 5µm (i); 1µm (j).

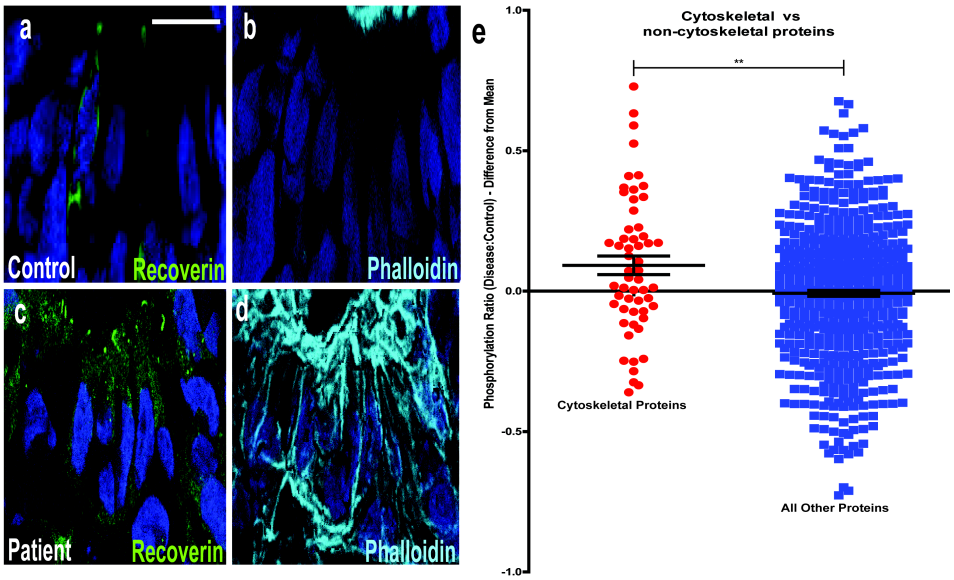

Figure 2. *RPGR*-mutant, iPSC-derived, 3-dimensional photoreceptor cultures display perturbed actin regulation. a-d: *RPGR*-mutant photoreceptors display increased actin polymerization, as evidenced by increased phalloidin binding in the Recoverin-positive photoreceptors of patient-derived cultures (panels c and d) as compared to photoreceptors from the control patient (panels a and b). See text for details of quantification of pixel intensities. Nuclei stained with Hoechst (blue) **e:** The mean phosphorylation level of cytoskeletal regulatory proteins was higher in *RPGR*/XLRP photoreceptors compared to control photoreceptors (red dots; 0.092 +/- 0.0033, n=56 proteins). This was significantly more than the mean ratio of phosphorylation levels of non-cytoskeletal proteins when *RPGR*/XLRP photoreceptors were compared to control (blue dots; -0.008 +/- 0.01, n=583 proteins, unpaired, two-tailed t test, p=0.004 (**=p<0.01)).

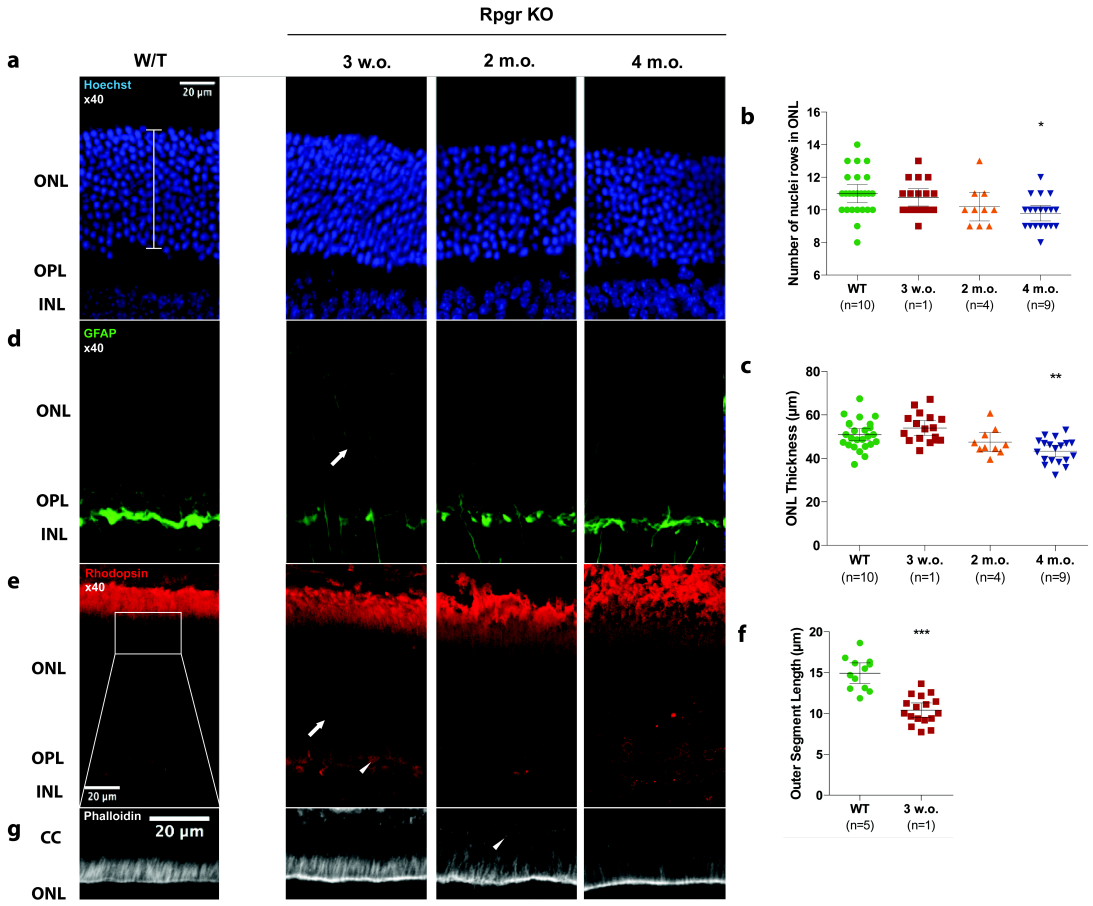

Figure 3. The *Rpgr* KO mouse retina demonstrates actin dysregulation and rhodopsin mislocalisation in the photoreceptor layer prior to degeneration. a-c: Outer nuclear layer (ONL - photoreceptor) degeneration develops in the *Rpgr* KO mouse (bracket represents the region measured). This change is significant by 4 months of age (compared to 4 month old wild type) as indicated by the number of rows of photoreceptor nuclei (**b**; Figures denote mean +/- SEM, Kruskal-Wallis test [H=30.8, 4d.f., p<0.0001], Dunn's multiple comparisons test, p<0.05, *=p<0.05) and ONL thickness (**c**; Figures denote mean +/- SEM, one-way ANOVA [F(4,76) = 10.7, p<0.0001], Tukey's multiple comparisons test, p<0.01 **=p<0.01). The WT control shown is 4 months of age. **d,e:** Reactive gliosis as reflected by increased GFAP immunolabeling throughout the radial length of Müller cells in the ONL is apparent as early as 3 weeks of age (arrow; **d**) whilst rhodopsin, normally only present in the outer segments outside (above in the figure) the ONL, is now mislocalised into other regions of the photoreceptor in the outer plexiform layer (OPL - arrowhead; e) and perinuclear area (arrow; **e**) at this timepoint, prior to the visible onset of photoreceptor degeneration. **f:** Outer segment length is reduced by three weeks of age (compared to 4 month old wild type; Figures denote mean +/- SEM, ***=p<0.001) after which they become markedly disorganised. **g:** Increased F-actin is seen in the connecting cilium (arrowhead) of the *Rpgr* KO mouse photoreceptor compared to wild type (Images representative of n=1-10 analysed).

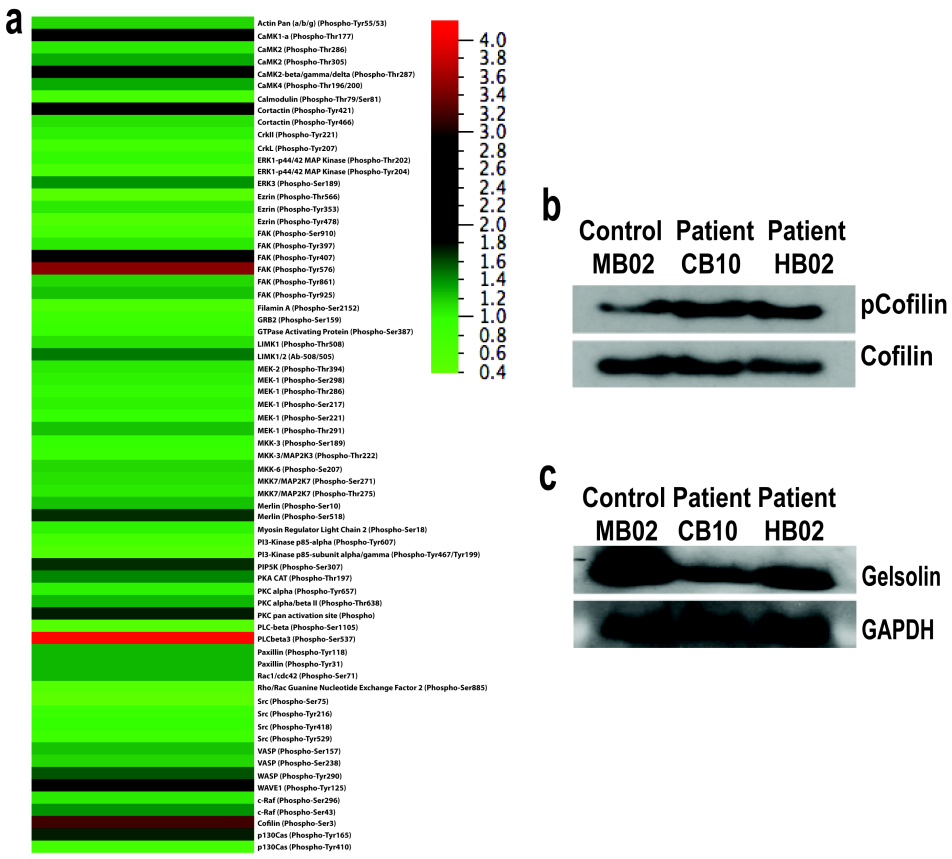

Figure 4. Studies of iPSC derived photoreceptor cultures reveals perturbation of gelsolin and cofilin activity in *RPGR* mutant lines. a: A phosphoarray comparing phosphorylation levels of cytoskeletal proteins in patient and control photoreceptor cultures identified cofilin as hyperphosphorylated on Serine 3 in *RPGR*-mutant photoreceptors (results presented as a heat map, with a patient:control ratio of phosphorylation for cofilin of 3.16). Note that only 3 other proteins (cortactin, FAK and PLCbeta3) show similar levels of hyperphosphorylation. **b:** This increase in cofilin phosphorylation was confirmed by western blotting of repeat cultures using a phospho-serine 3 specific antibody. **c:** F-actin-bound (active) gelsolin is reduced in *RPGR*-mutant photoreceptors.

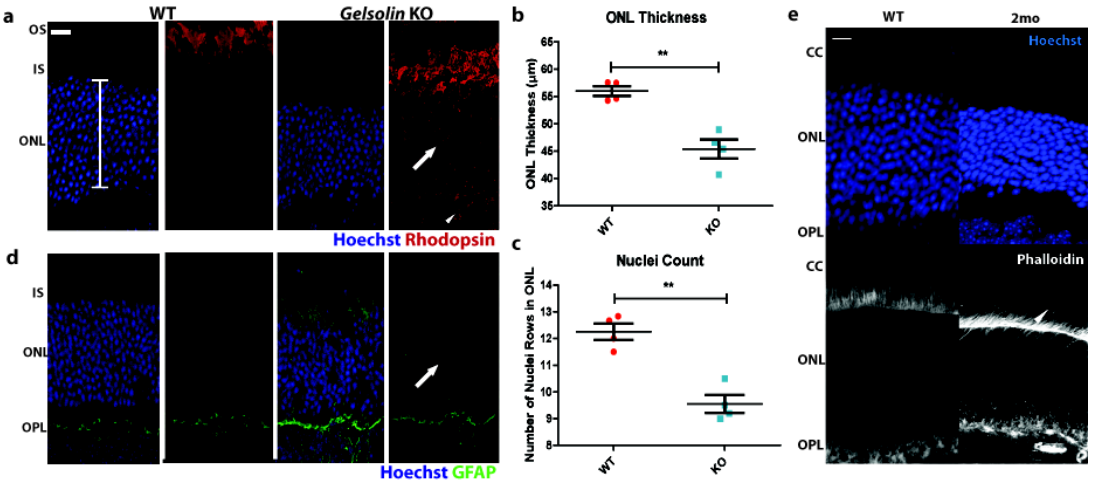

Figure 5. Knock out mouse studies confirm a role for Gelsolin in photoreceptor maintenance. a-c: Outer nuclear layer (ONL) degeneration develops in the *gelsolin* knock out mouse at 5 months of age (**a**; bracket represents ONL length measured); significant for ONL thickness (**b**; n=4, Figures denote mean +/-SEM, unpaired two-tailed t-test, **=p<0.01) and rows of nuclei (**c**; n=4, Figures denote mean +/-SEM, unpaired two-tailed t-test, **=p<0.01). As in the *Rpgr*-KO mouse shown in Fig. 3, rhodopsin is mislocalised to the outer plexiform layer (arrowhead; **a**) and perinuclear area (arrow; **a**). **d:** Increased GFAP immunolabeling throughout the radial length of Müller cells in the ONL is apparent (arrow) at 5 months of age. **e:** Increased F-actin is seen in the connecting cilium (arrow head) of *Gelsolin* KO mouse photoreceptor compared to wild type. (Images representative of n=3 analysed). Scale bars: 20µm (**a,e**)

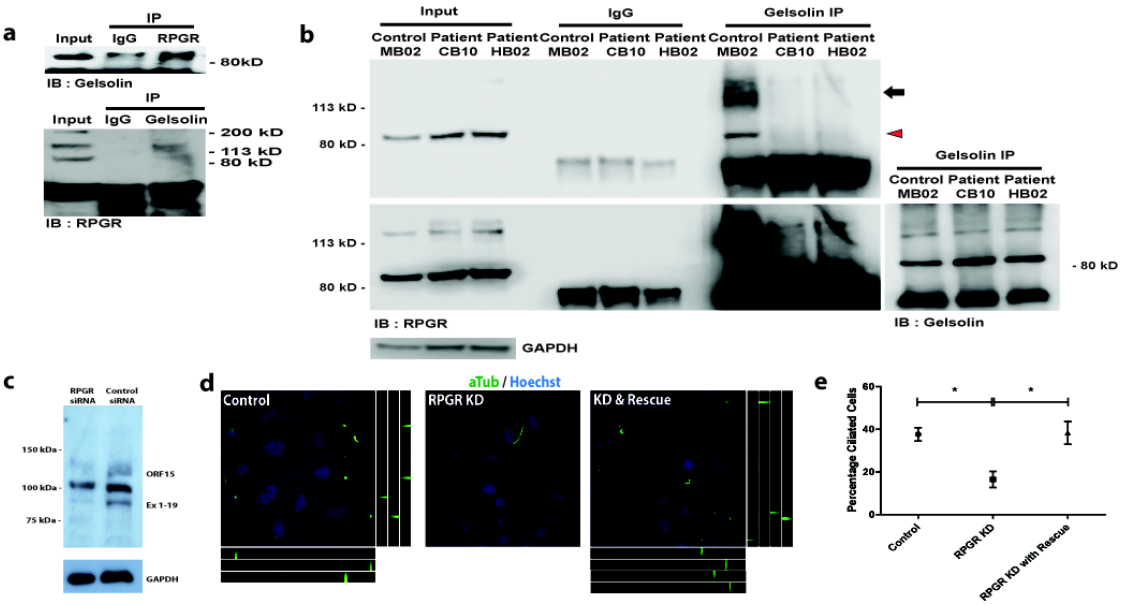

Figure 6. Loss of function and gain of function experiments support a role for gelsolin in *RPGR* mediated cilia maintenance. a: Immunoprecipitation (IP) of RPGR (upper panel) and gelsolin (lower panel) demonstrates an endogenous RPGR-gelsolin interaction in bovine retina, as evidenced by immunoblotting (IB) showing the presence of gelsolin (86kD) and the 127kD retina-specific form of RPGR respectively in the immunoprecipitates. **b:** Immunopreciptation (IP) of gelsolin followed by immunoblotting (IB) for RPGR reveals that the RPGR-gelsolin interaction is present in control iPSC-derived photoreceptors but is perturbed in both XLRP patient-derived *RPGR*-mutant cultures – note in the righthand set of three lanes that RPGR is present only in the IPs from the control patient. The lower panel shows a longer exposure of the immunoblot to show that both the constitutively-expressed (90kD, encoded by exons 1-19, arrowhead) and retina-specific (127kD – encoded by exons 1-14 and specific open reading frame ORF 15, arrow) forms of RPGR are present in the control and mutant cell lysates shown in the three left hand lanes. Far right panel shows equal amounts of gelsolin are pulled down from each sample by gelsolin IP. **c:** siRNA-mediated *RPGR* knock down. Note that expression of both the both the constitutively-expressed (90kD – Ex 1-19) and retina-specific (127kD – ORF 15) forms of RPGR are reduced by the siRNA while the non-specific band at 100kD is unaffected) in the hTERT-RPE cell line. **d-e**: Immmunolabeling of the hTERT-RPE cell line after siRNA-mediated *RPGR* knock down reveals a loss of ciliogenesis (Mean percentage of ciliated cells 37.62%+/-3.113 v 16.48%+/-3.762 (SEM), unpaired two-tailed t-test, p=0.0124; identified by acetylated α-tubulin immunoreactivity in green), as shown by a comparison of the control (left) and *RPGR* knock down (centre) panels. The defect is rescued by overexpression of constitutively active gelsolin, as shown in the right panel (Mean percentage of ciliated cells 16.48% +/- 3.762 v 38.33% +/- 5.349 (SEM), unpaired two-tailed t-test, p=0.0288.) The tracks below and to the right of the micrographs in **d** show z-planes of the image to confirm the presence of elongated cilia. Scale bars: 10μm (**d**).

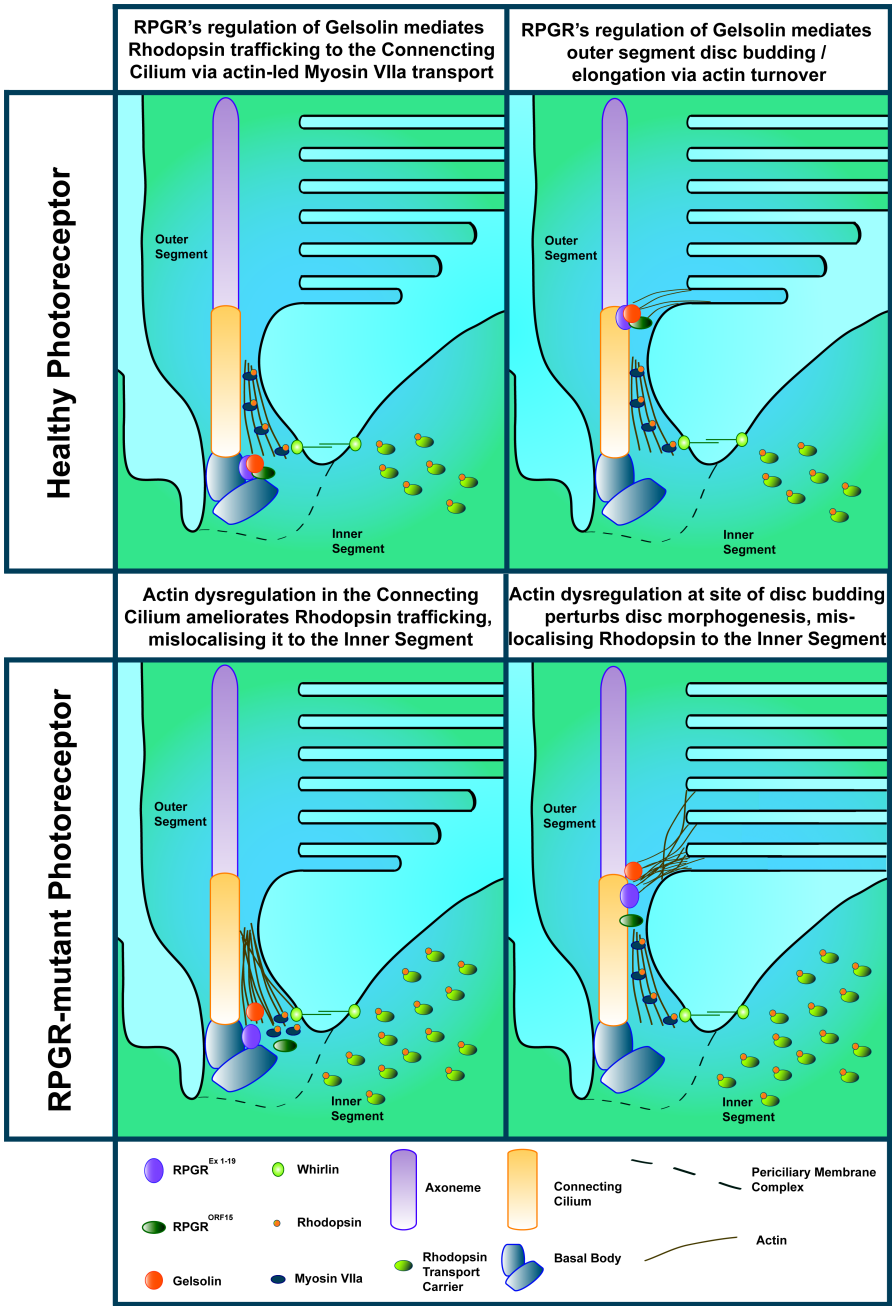

Figure 7. Proposed model for RPGR mediated actin turnover in the photoreceptor connecting cilium. We propose two possible mechanisms of action for RPGR. Firstly, RPGR's regulation of actin turnover could mediate rhodopsin trafficking into the photoreceptor connecting cilium (left panels). An actin bundle connects the periciliary membrane complex to the basal body, along which Myosin VIIa actively transports visual pigments. Whirlin regulates this actin network at the connecting cilium base and interacts with both gelsolin and RPGR, suggesting a model whereby mutant RPGR disrupts the complex, perturbing actin turnover and compromising Myosin VIIa-mediated rhodopsin transport (left panels). The resulting rhodopsin mislocalisation to the inner segment results in cell stress and degeneration. Secondly, RPGR's regulation of actin turnover could facilitate outer segment disc formation (right panels). Actin exerts an influence on both ciliogenesis and maintenance and is localised to the site of photoreceptor disc budding. The disorganised discs and hyperstabilised actin seen in the Rpgr knock-out mouse supports a model whereby RPGR facilitates outer segment disc budding or the completion of disc formation via gelsolin-mediated actin turnover (right panels). The compromised disc morphogenesis seen with mutant RPGR would mislocalise rhodopsin to the inner segment, resulting in cell stress and degeneration.

Supplementary Information

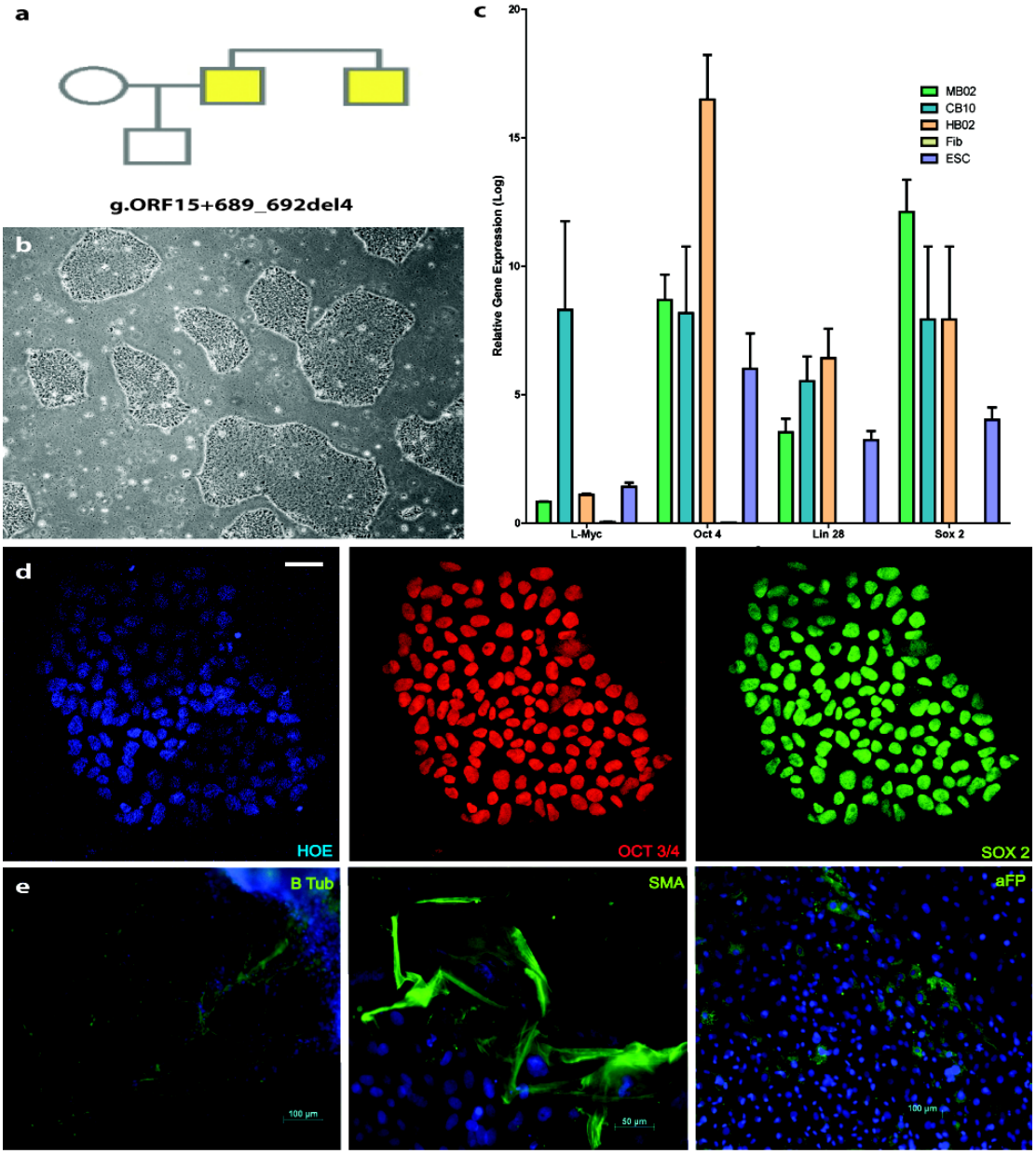

Supplementary Figure 1. iPSC generation from a family with an *RPGR* mutation. a: Two brothers with g.ORF15+689_692del4 mutations in *RPGR* and their unaffected son/nephew underwent skin biopsies. **b:** iPSC colonies were expanded following nucleofection with transgenes (see methods). **c:** qPCR demonstrated high endogenous expression of pluripotency markers in all cell lines used in this paper compared to fibroblasts (Fib) and the H9 embryonic stem cell line (ESC). **d:** Immunohistochemistry demonstrated the expression of pluripotency markers (OCT4, SOX2) in iPSC colonies. **e:** iPSC lines were pluripotent as demonstrated by their ability to differentiate down all three germ layers to form ectoderm (β-Tub staining), mesoderm (SMA staining) and endoderm (αFP staining). (Images representative of n=3 analysed). Scale bar: 10µm (d)

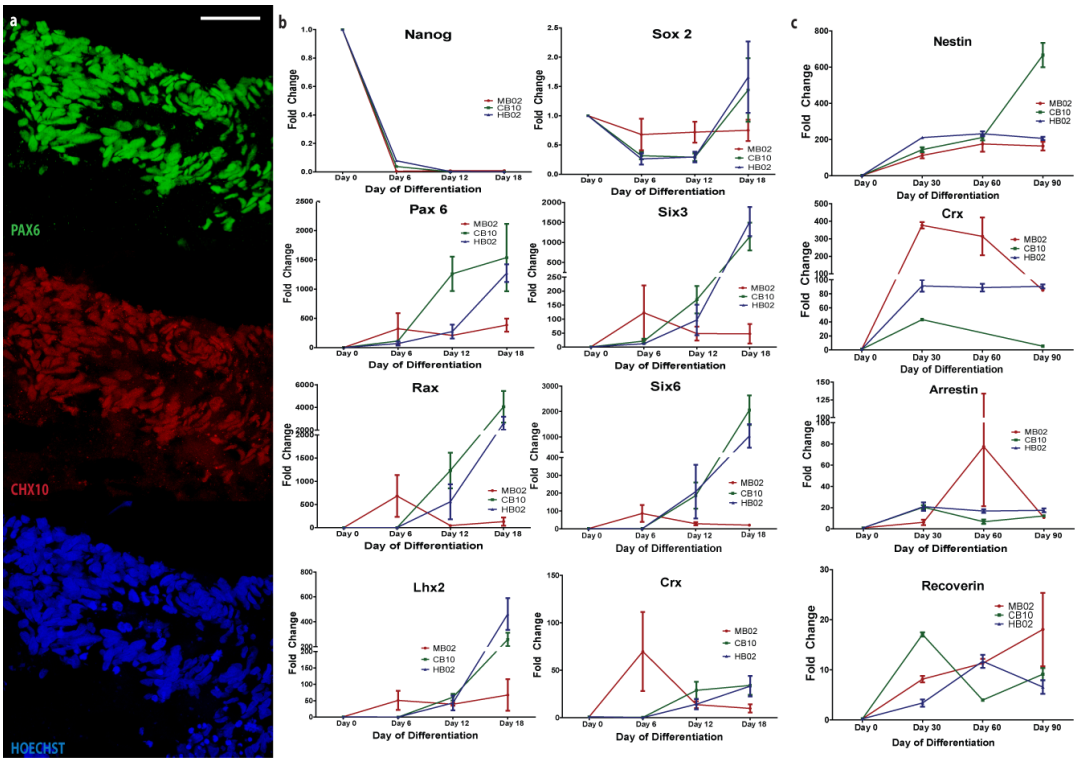

Supplementary Figure 2. Further characterization of iPSC derived 3 dimensional photoreceptor cultures. a: Successful patterning of free-floating aggregates resulted in PAX6^{+}/CHX10^{+} regions developing by day 10 (Images representative of n=3 analysed). **b:** qPCR demonstrated the loss of pluripotency in cultures, with *NANOG* downregulation observed by day 12 of differentiation. *SOX2* expression persisted and *PAX6* expression increased as cultures became neuralised. Upregulation of the eye field genes *RAX, SIX3, SIX6, LHX2* and *CRX* occurred in all three iPSC lines indicating successful eye field patterning. **c:** qPCR at later timepoints during photoreceptor differentiation showed persistence of neural markers (*Nestin*) alongside upregulation of mature photoreceptor genes (*Arrestin, Recoverin*). Scale bar: 20μm (a)

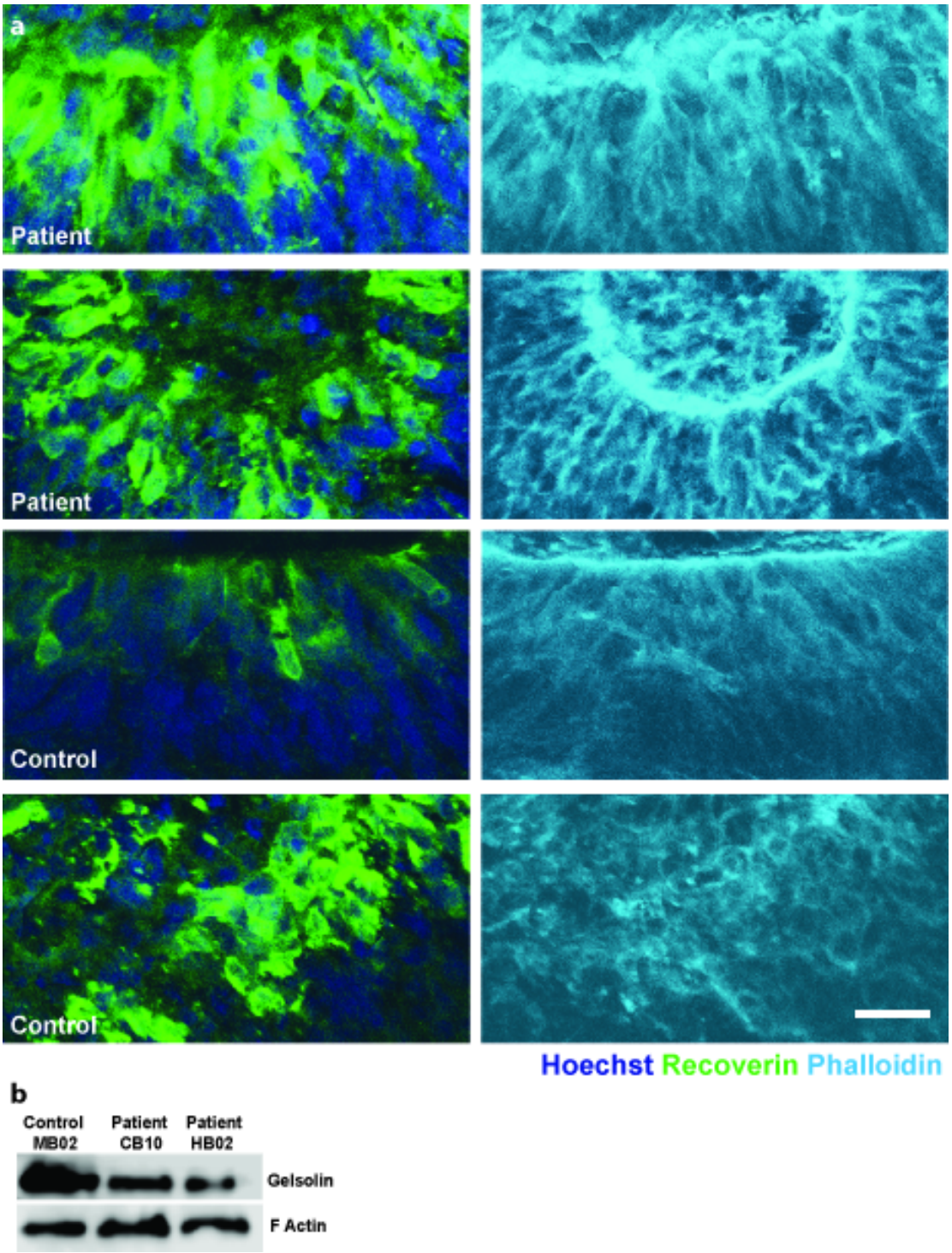

Supplementary Figure 3. *RPGR* mutant, iPSC derived, 3 dimensional photoreceptor cultures display perturbed actin regulation and reduced gelsolin activation. a: *RPGR*-mutant photoreceptors display increased actin polymerization, as evidenced by increased phalloidin staining in the recoverin-positive photoreceptors of patient-derived cultures (top 2 panels) as compared to photoreceptors from the control patient (bottom 2 panels) (Images representative of n=3 analysed).. **b:** F-actin-bound (active) gelsolin is reduced in *RPGR*-mutant photoreceptors, when normalized against actin.

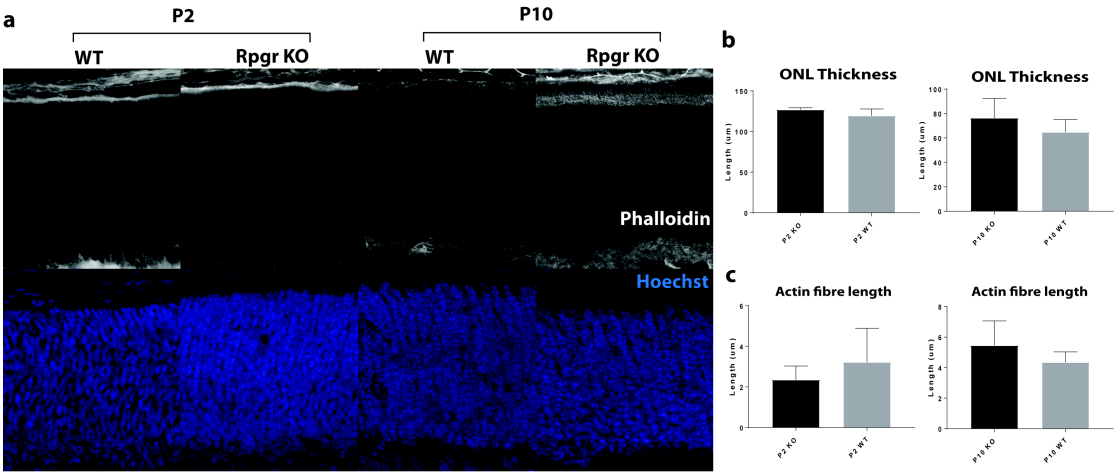

Supplementary Figure 4. The developing *Rpgr* KO mouse retina demonstrates no outer nuclear layer developmental abnormality or actin dysregulation prior to eyes opening. a,b: No outer nuclear layer (ONL - photoreceptor) abnormality is seen in the developing *Rpgr* KO mouse at post natal day 2 (P2) or 10 (P10) (compared to P2 and P10 wild type retina, respectively; Figures in **b** denote mean +/- SEM, one-way ANOVA). **a,c:** Actin bundles extending from the outer plexiform layer to the base of the connecting cilium are not significantly different in length at post natal day 2 (P2) or 10 (P10) in the KO mouse (compared to P2 and P10 wild type, respectively; Figures denote mean +/- SEM, one-way ANOVA). (Images representative of n=3 analysed).

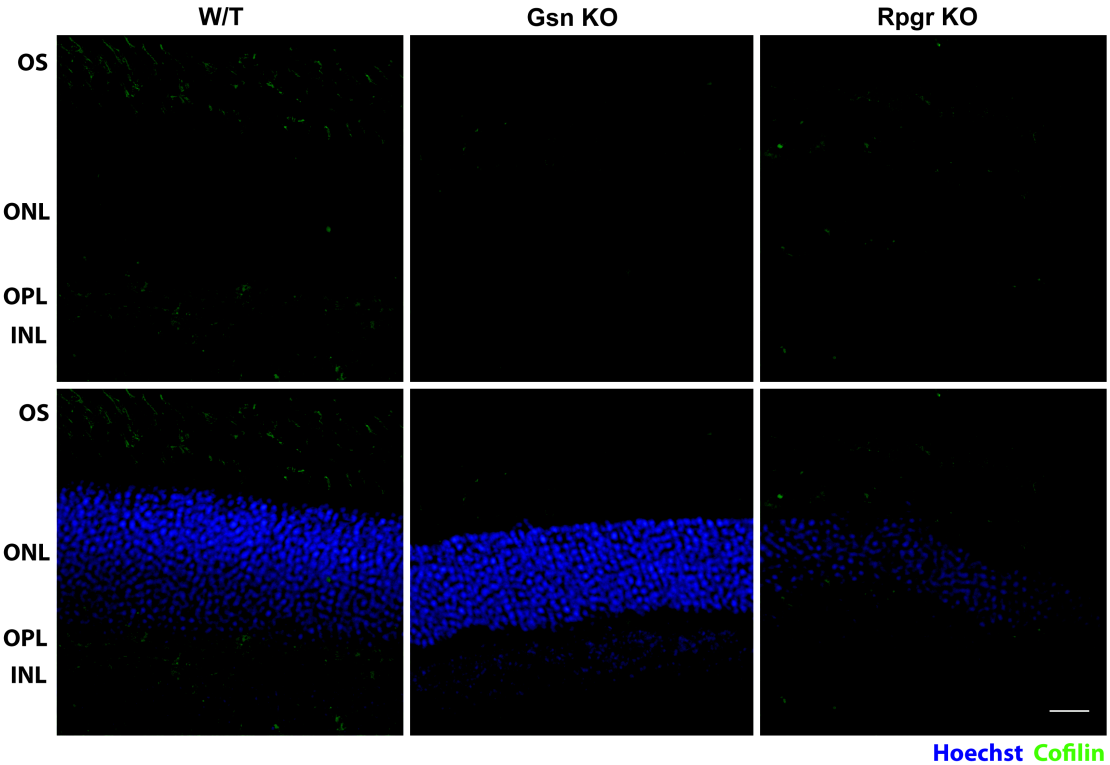

Supplementary Figure 5. Cofilin localization in the murine retina. Cofilin localizes to the photoreceptor outer segments (OS) and outer nuclear layer (ONL) in mature wild type murine retina. This localization is not altered in *Rpgr* KO or *Gelsolin* KO retina. (Images representative of n=3 analysed). Scale bar: 30µm

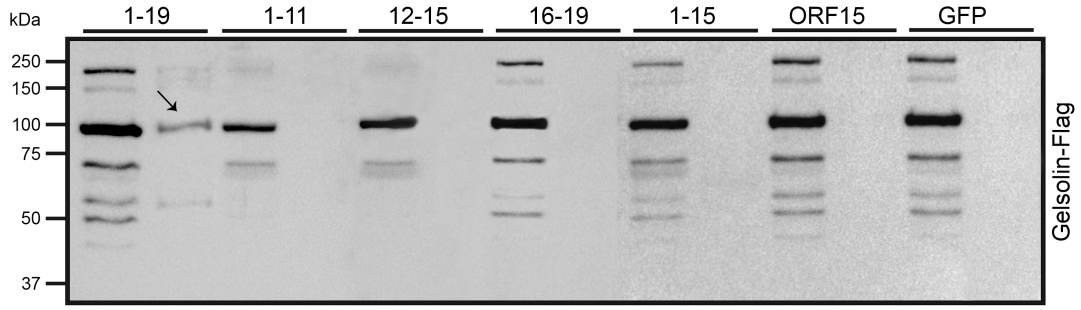

Supplementary Figure 6. Gelsolin directly interacts with the constitutive RPGR^{Ex1-19} splice variant. RPE1 cells transiently transfected with FLAG-Gelsolin and indicated GFP-RPGR encoding constructs were subjected to IP using GFP antibody. The precipitated proteins were analyzed by SDS-PAGE and immunoblotting using FLAG (antibodies. Cells expressing GFP tag alone were used as negative control. Arrow indicate specific immune-reactive bands.

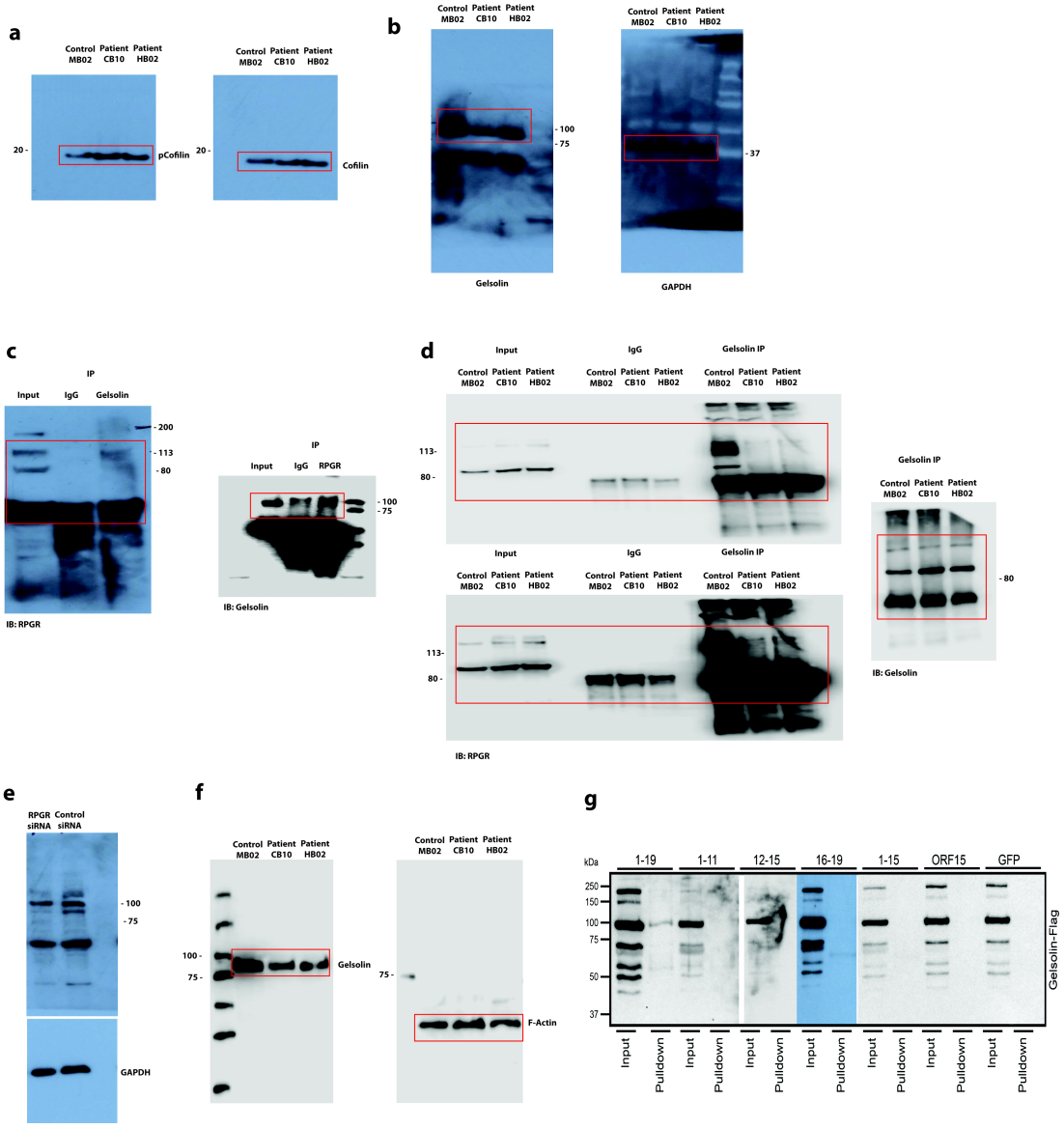

Supplementary Figure 7. Uncropped scans of the Western blot and Co-immunoprecipitation images seen in **a:** Figure 4b; **b:** Figure 4c; **c:** Figure 6a; **d:** Figure 6b; **e:** Figure 6c; **f:** Supplementary Figure 3b; **g:** Supplementary Figure 6.